Article

Fullerene-Filtered Light Spectrum and Fullerenes Modulate Emotional and Pain Processing in Mice

Jelena Lazovic [1,*], Lydia M. Zopf [2], Jernej Hren [3], Martin Gajdoš [4], Marija Slavkovic [5], Zorana Jovic [5], Ivana Stankovic [6], Valentina Matovic [6] and Djuro Koruga [5]

[1] Medical Systems Central Scientific Facility, Max Planck Institute for Intelligent Systems, 70569 Stuttgart, Germany
[2] Ludwig Boltzmann Institute for Experimental and Clinical Traumatology, 1200 Vienna, Austria; lydia.zopf@trauma.lbg.ac.at
[3] Lek Veterina d.o.o., 9231 Beltinci, Slovenia; jernej.hren@lek-veterina.si
[4] Neuroscience Center, CEITEC—Central European Institute of Technology, Masaryk University, 625 00 Brno, Czech Republic; martin.gajdos@ceitec.muni.cz
[5] TFT Nanocenter, 11000 Belgrade, Serbia; marija.slavkovic@tftnanocenter.rs (M.S.); zorana.jovic@tftnanocenter.rs (Z.J.); djuro.koruga@tftnanocenter.rs (D.K.)
[6] NanoLab, Biomedical Engineering, Faculty of Mechanical Engineering, University of Belgrade, 11000 Belgrade, Serbia; imileusnic@mas.bg.ac.rs (I.S.); vmatovic@mas.bg.ac.rs (V.M.)
* Correspondence: zinnanti@is.mpg.de; Tel.: +49-660-670-9665

Abstract: The most symmetric molecule, Buckminster fullerene C_{60}, due to its unique properties, has been intensively studied for various medical and technological advances. Minimally invasive and minimally toxic treatments hold great promise for future applications. With this in mind, this research exploited the physical properties of fullerene molecules for potential therapeutic effects. Pristine fullerenes have peak absorbance in the 380–500 nm range, making them an attractive violet-blue light filter. Since spectral quality of light can affect behavior, this research used resting state functional magnetic resonance imaging (rs fMRI) and behavioral testing to directly evaluate the effects of fullerene-filtered light on brain processing and behavior in mice. The same method was used to study if hydroxyl fullerene water complexes (3HFWC), with or without fullerene-filtered light, modulated brain processing. A month-long, daily exposure to fullerene-filtered light led to decreased activation of the brain area involved in emotional processing (amygdala). Water supplemented with 3HFWC resulted in an activation of brain areas involved in pain modulation and processing (periaqueductal gray), and decreased latency to first reaction when tested with a hot plate. The combination of fullerene-filtered light with 3HFWC in drinking water led to restored sensitivity to a hot plate and activation of brain areas involved in cognitive functions (prelimbic, anterior cingulate and retrosplenial cortex). These results uncovered the potential of fullerene-filtered light to impact emotional processing and modulate pain perception, indicating its further use in stress and pain management.

Keywords: fullerene; fullerenol; fullerenol water complex; emotional processing; anxiety; light spectrum; pain; resting state fMRI; MRI; behavior

1. Introduction

Since the discovery of the icosahedral form of carbon [1], fullerenes have attracted considerable interest in many fields of research, including biomedical applications. Their unique carbon cage structure, potential to readily react with free oxygen radicals and peak absorption in the UV-blue range makes them suitable for various purposes including drug delivery, antioxidants, anti-aging, anti-inflammatory as well as defense against UV-radiation [2–7]. Novel uses are constantly emerging thanks to innovative ways to exploit their physical and chemical properties, yielding a variety of therapeutic agents. The widespread biomedical application of fullerenes began with the advent of a hydroxylated

form of fullerene [8] and water-soluble fullerenes [9]. The addition of more hydroxyl groups and water molecules made polyhydroxylated fullerene [8] highly water soluble [10].

In recent years, accumulating evidence suggests the spectral quality of light plays a role in behavioral processing that does not involve image formation, such as alertness, mood regulation and cognitive functions [11,12]. This mechanism is attributed to the melanopsin-expressing intrinsically photosensitive retinal ganglion cells (ipRGC) [13–15], via their widespread projections to the brain [16,17]. These cells represent the third class of retinal ganglion cells, believed to be the principal conduits for rod/cone input to the non-image forming (NIF) vision [18]. Mice devoid of rod and cones photoreceptors are still capable of circadian entrainment, presumably via changes in spectral irradiance detected by ipRGCs [19–22]. Moreover, it was demonstrated that changes in spectral composition (colors) throughout the day are more important for synchronizing biological clocks than the intensity of irradiance alone [23]. It appears that ipRGCs, innervated by rods and cones, contribute to the entrainment of the circadian system by combining both environmental irradiance and spectral information. In addition, more evidence now suggests the spectral composition of light to influence many other processes such as melatonin secretion, corticosteroid levels, alertness, fertility, mood changes, sleep and to play a role in psychiatric disorders [11,24–26]. In particular, many mental illnesses are thought to be associated with circadian rhythm disruption including attention deficit hyperactivity disorder (ADHD), bipolar disorder, depression, schizophrenia and addiction [27–31]. It is still unclear whether these disturbances are caused by an inability to properly regulate circadian rhythm, or whether changes in light spectral composition via artificial lighting (presumably dominated by blue light) can have long-term behavioral alterations. Other indications suggest that spectrum devoid of blue light can lead to depression [32]. This is not surprising, since peak absorption of melanopsin is ~479 nm, making ipRGC exclusively sensitive to blue light [33]. Therefore, it is conceivable that light composition with dominating blue wavelengths (LED light), or completely devoid of blue light can lead to various disturbances. Nano size fullerene particles have peak absorption between 380 and 500 nm [34], acting as an optical filter in violet, blue and green regions, with the ability to moderate the intensity of these colors. However, in order to more effectively utilize fullerene-filtered light for therapeutic purposes, it is first necessary to determine the effects of various spectral compositions on brain processing and behavior. Using resting state functional MRI (fMRI) and behavioral testing, changes in brain activity and behavior in response to fullerene-filtered light were directly determined. fMRI is a widely accepted non-invasive method to investigate brain function in response to stimulus. It has been established, that following brain activation, oxygenated blood is quickly delivered to activated regions to replenish the increased demand for oxygen [35,36]. Therefore, activated brain areas can be detected indirectly by measuring the increase in MRI signal (directly correlated with the increase in oxygenated blood [35,36]). When the brain is at rest, different brain regions receive different oxygen supplies, however, it appears that the level of oxygen supply is synchronized throughout the brain, and this synchrony can be measured as an amplitude of low frequency fluctuation of the signal (ALFF) [37]. Different stressors coming from the environment, diet, pharmacological agents or mental illnesses can all lead to disruption of the synchrony and manifest as changes in ALFF signal. Therefore, by comparing ALFF signal between control and treatment groups, it is possible to evaluate differences in patterns of brain activation. In contrast to functional MRI, where a task is performed during an MRI scan, resting state fMRI measures changes in brain activity at rest, and does not require any specific stimulus.

Fullerenes and their derivatives are expected to have diverse applications in the future, especially in medicine and neuroscience. Before more advanced therapies are designed, it is desirable to determine if and how they can affect normal brain function and behavior. Motivated to use minimally reactive fullerenes, in the form of hydroxylated fullerene water complex (3HFWC), the same methodology was used to determine brain activation and behavioral changes as a ground for future applications.

2. Materials and Methods

2.1. Materials

An OSRAM (Osram GmbH, Germany) halogen light, with specific power density 40 mW/cm^2 (from a distance of 10 cm), light energy density 2.4 J/cm^2 per min, integrated inside a Bioptron-compact device (BIOPTRON AG, Switzerland), was used as a source of halogen light. This device produces polychromatic, non-coherent linearly polarized light (via a Stoletov glass pile placed at a Brewster angle) with wavelengths 320–3400 nm. The fullerene filter, 2 mm thick, was made from polymethyl methacrylate (PMMA) glass with the addition of 0.3% fullerene (PMMA-C$_{60}$) [38–41]. The power density of light passed through the fullerene filter measured from a 5 cm distance was 55–65 mW/cm^2. This fullerene filter is also commercially available (BIOPTRON AG, Switzerland). Characterization of the spectral characteristics of halogen and fullerene-filtered halogen light were performed using a high resolution spectrometer (QE Pro, Ocean Insight, Orlando, FL, USA), Figure 1A,B. During the light treatment, room lights were turned off, and the only light exposure was from the halogen light, or fullerene-filtered light, Figure 1C.
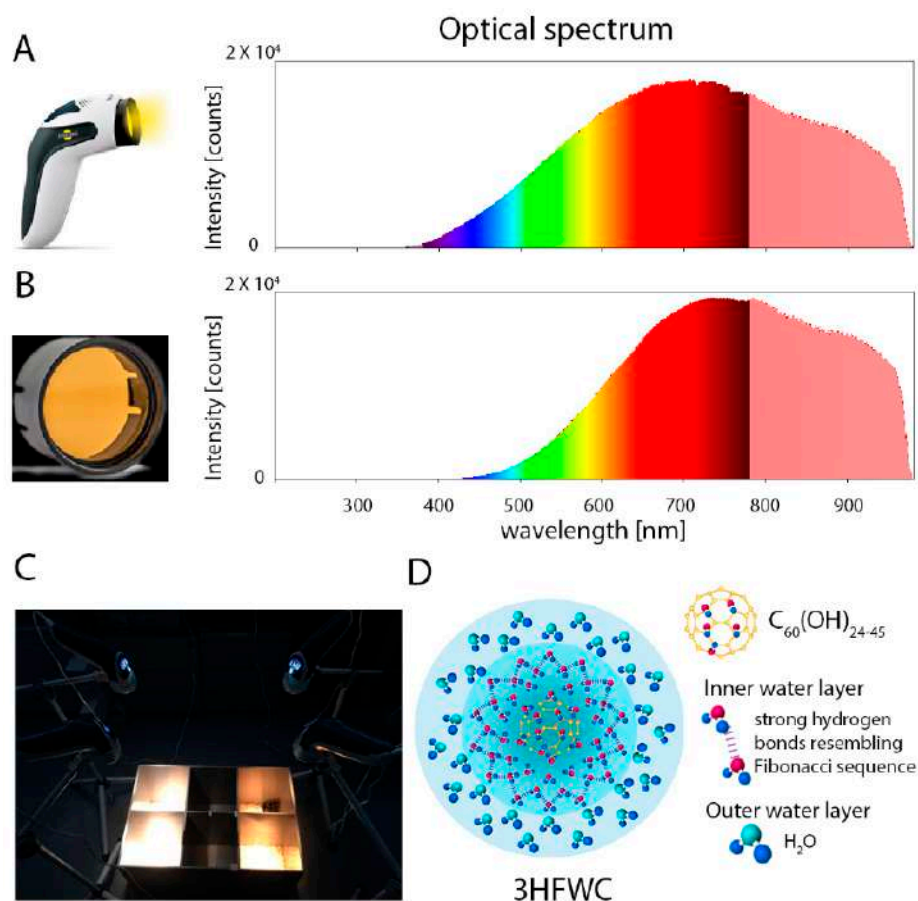

Figure 1. Measurement of: (**A**) halogen light (BIOPTRON device) optical spectrum, and (**B**) fullerene-filtered halogen light spectrum (adjusted for distance to lead similar intensity counts, so that light composition can be easily compared). (**C**) Experimental setup of light exposure. All mice were treated simultaneously in a dark room. (**D**) Illustration of aqueous fullerene water complex (3HFWC) used in the study, with a fullerene molecule in the middle, attached hydroxyl groups (OH), surrounded by water molecules interacting with weak hydrogen bonds.

The fullerenol [C$_{60}$(OH)$_{24–45}$] was purchased from Solaris Chem Inc, Vaudreuil-Dorion, Quebec, Canada. Hydroxyl modified fullerene water complex (3HFWC) was made by mixing fullerenol [C$_{60}$(OH)$_{24–45}$] with ultrapure water (0.05 μS/cm). The water layers were generated and stabilized by an oscillatory magnetic field [C$_{60}$(OH)$_{24–45}$.H$_2$O)$_{144–2528}$],

leading to stable hydroxylated fullerene water complexes 7–12 nm in diameter [42,43], Figure 1D. Before mixing with water, fullerenol was pre-treated in an ultrasonic apparatus (Stone Age Industries, Powell, WY, USA) to prevent agglomeration and aggregation.

2.2. Animals

Male mice (*Mus musculus*, C57Bl/6JRj, 8 weeks old) were purchased from a commercial breeder (Janvier Labs, Le Genest-Saint-Isle, France). All animal procedures were performed in accordance with institutional guidelines, 2010/63/EU directive of the European Parliament, and were approved by an Austrian authority (BMWFW), license number BMWF66.015/0010-V/3b/2018. All mice were housed under a 14:10 light:dark cycle. Treatment sessions began when mice were 11.5 weeks old. After 4 weeks of treatment, a resting state fMRI was performed, and daily treatments continued until behavioral tests were completed and for two weeks afterwards (additional 8 weeks). The light exposure treatment with halogen light or fullerene-filtered halogen light consisted of two sessions (morning and afternoon), each two hours long, for a total of four hours of daily light treatment. The 3HFWC was used orally alone or in combination with fullerene-filtered light. Mice were randomly divided into 4 groups, with *n* = 5 mice in each group. A control group (the first group) was exposed to halogen light and was given regular drinking water. The second group of mice was exposed to fullerene-filtered light and given regular drinking water. The third group was exposed to halogen light and given 3HFWC (0.15 g/L) supplemented drinking water. The fourth group of mice received dual treatment, exposed to fullerene-filtered light and given 3HFWC (0.15 g/L) in drinking water. During the light treatment with halogen or fullerene-filtered light, mice were placed in a box (15 × 15 cm) with a thin layer of bedding material, in groups of 5 (the original grouping as in their home cages) and were allowed to freely move and interact, Figure 1C. All mice had access to food and water (regular or 3HFWC supplemented) ad libitum, except during the light exposure treatment, which was performed without access to food or water. Starting at 10.5 weeks of age, mice were weighed (S94792A, Fischer scientific, Waltham, MA, USA) weekly for 7 weeks. Blood pressure was monitored weekly (Coda system, Kent Scientific, Torrington, CT, USA), along with ECG (SA Instruments Inc, Stoony Brook, NY, USA).

2.3. Behavioral Testing

Prior to behavioral testing, mice were transferred to the behavioral facility and allowed one week for habituation to the new environment. All data from behavioral studies were analyzed by a person blind to the experimental groups.

2.3.1. Elevated Plus Maze

Mice were placed in the center zone (6.5 × 6.5 cm^2), facing the open arm of a custom-built elevated plus maze (elevated 54 cm above the floor) with 2 open arms (OA, 30 cm length, 7 cm width) and 2 wall-enclosed arms (closed arms, CA, 30 cm length, 6 cm width, walls 14.5 cm high) and allowed to freely explore for 5 min. The sessions were videotaped, recorded and analyzed using Topscan software (Cleversys, Inc., Reston, VA, USA). The latency to enter open arms, time spent in open arms, and distance travelled in open arms were evaluated.

2.3.2. Forced Swimming Test (Porsolt Test)

Mice were placed individually into a 2 L glass beaker filled with water at room temperature (24 ± 1 °C), and videotaped. The amount of time mice spent floating as opposed to swimming and struggling, and the onset of floating or immobile posture were measured during a 6 min session. Adopting an immobile posture during the test was interpreted as giving up. During the 6 min period, mice were constantly watched to prevent drowning. Following the test, mice were placed under an infrared lamp until they were dry.

2.3.3. Tail Suspension Test

Mice were taped to a rod by their tails and left dangling heads down for 6 min [44]. The latency until the mouse ceased all efforts to adopt an upright position was measured.

2.3.4. Hot Plate Test

Thermal sensitivity was tested using a hot plate analgesia meter (IITC Life Science Inc., Woodland Hills, CA, USA). Mice were put on the hot plate at 52 °C. The experiment was stopped as soon as the mice performed their first jump. Mice were videotaped and the latency and the temperature of their first reaction (hind paw shaking or licking) or jump were recorded.

2.3.5. Dynamic Plantar (von Frey) Test

Touch sensitivity was tested with a dynamic plantar aesthesiometer (Ugo Basile S.R.L., Gemonio, Italy) and an automatic von Frey test [45,46]. Mice were habituated to the testing chambers (metal grid) for approximately 2 h prior to testing. Each hind paw was tested for touch sensitivity by poking the plantar surface with a von Frey filament of a given diameter with a force that increased from 0 to 10 g within 20 s. There were at least 20 s between each trial on the same mouse. The maximum force of 10 g was never exceeded. The average of 3 trials was calculated for each hind paw. The force and latency at which the mouse lifted the hind paw were recorded.

2.3.6. Nest Building Test

For the nest building test, mice were single-housed for one night in a clean cage containing a standardized cotton nestlet that could be used for nest building. The next morning the quality of the nest (using a 5-point nest-rating scale) and the amount of used nestlet material was evaluated as previously described [47]. In brief, a score (between 1 and 5) was given, 1 = nestlet not noticeably touched (more than 90% intact), 2 = nestlet partially torn (50–90% remaining intact), 3 = nestlet mostly shredded, but not identifiable nest, 4 = an identifiable nest (more than 90% of the nestlet is torn, but the nest is flat with short or no walls), 5 = a nearly perfect nest in the shape of a cocoon with walls and partial or complete roof. The unused nestlet material was weighed, and the weight subtracted from the original weight in order to calculate used nestlet material.

2.4. Statistics

Data sets from behavioral studies were first checked for normal distribution, and then analyzed by one-way analysis of variance (ANOVA) followed by Fisher's LSD post-hoc test. Origin (Origin 2019b Pro version, OriginLab Corporation, Northampton, MA, USA) was used for statistical analysis. All p-values less than 0.05 were considered statistically significant.

2.5. Resting State Functional MRI (rs-fMRI)

Functional imaging was performed using 15.2 T small animal MRI (Bruker BioSpec, Ettlingen, Germany) and with 23 mm birdcage coil. Prior to imaging, all mice were anesthetized with 4% isoflurane for initial sedation induction and immediately reduced to 2%. During imaging, adjustments to the isoflurane concentrations were made, so that respiration did not fall below 140 breaths per minute (bpm) at any time. For the resting state fMRI study, a single shot echo planar imaging (EPI) sequence with spin echo readout was used (TR = 2000 ms, TE = 19.7 ms, FOV = 16×16 mm^2, number of excitations (NEX) = 1, voxel size = 250×250 μm^2, 30 slices, slice thickness 0.5 mm, 360 repetitions, 12 min total imaging time). After functional scans, high-resolution T$_1$-weighted images were acquired using a gradient echo sequence (TR = 500 ms, TE = 3 ms, FOV = 16×16 mm^2, NEX = 4, voxel size = 125×125 μm^2, 30 slices 0.5 mm thick) for the anatomical co-registration.

2.5.1. Data Processing for Resting State fMRI

Resting state fMRI data were processed using the Data Processing Assistant for Resting-state fMRI Advanced Edition (DPARSF-A) toolbox, which is part of the Data Processing and Analysis of Brain Imaging (DPABI) toolbox version 2.1 (http://rfmri.org/dpabi accessed on 12 October 2021) [48]. Prior to the analysis, the initial 10 scans were discarded (to assure magnetization has reached steady state). Standard pre-processing procedures including corrections for slice-timing, realignment, co-registration, normalization, and segmentation were conducted using DPABI toolbox. To reduce the interference of physiological noise, mean time-series from white matter (WM) and cerebrospinal fluid (CSF) were used as nuisance regressors in the general linear model [49]. Friston 24-parameter model was used to regress out nuisance covariates related to motion [50]. A spatial smoothing was performed using 2.4 pixel full-width half-maximum Gaussian kernel. A band pass filter (0.01–0.1 Hz) was applied following nuisance regression and smoothing. Anatomical scans and functional images were co-registered to the in-house generated mouse atlas with 80 distinct brain regions. The amplitude of low frequency fluctuation (ALFF) was used to determine regions of activation [51]. For each mouse ALFF map was calculated and z-transformed (z-score ALFF map) for statistical analysis.

2.5.2. Group Level Analysis for rs-fMRI

The between comparison between experimental and control group was conducted on z-scored ALFF maps, using pairwise t-test followed by Gaussian Random Field (GRF) theory for multiple comparison correction (voxel-level p-value = 0.05, cluster-level p-value = 0.05). Data were analyzed with and without linear regression of global signal [52–54]. Resting state fMRI results with global signal regression (GSR) were presented.

2.6. Histology

At the end of treatments, which lasted 12 weeks in total, mice were sacrificed by cervical dislocation. The heart, lung, liver spleen, kidney, brain, bone and skeletal muscle tissue were dissected from each animal and immediately fixed in 10% Normal Buffer Formalin (Leica, cat. 3800600) for 16 h. Samples from 3 animals of each group were chosen for further processing (paraffin embedding) and evaluation. From each paraffin block, 2 μm thick sections were cut and the tissue was stained using H&E and slide stainer Microm HMS 740 (Thermo Scientific), except for the brain. For brain slides, Luxol Fast Blue (using 0.1% Solvent Blue, Sigma cat. 229121) and Cresyl Violet (Sigma cat. C5042) stainings were performed. Stained slides were examined under a Zeiss Axioskop 2 MOT microscope (Carl Zeiss Microscopy Deutchland GmbH, Oberkochen, Germany) and scanned with a Pannoramic 250 Flash II Scanner (3D Histech, Budapest, Hungary).

3. Results

Use of a fullerene optical filter in front of a halogen light, led to reduction of light intensity in the violet, blue and green regions, as expected, (Figure 1A,B), producing the characteristic "fullerene-filtered light spectrum". Accumulating evidence implicates a connection between mood disorders, depression and sleep disturbances with light spectral composition [32]. Since increased light intensity in the blue region, as well as absence of blue light from the spectrum, can modulate emotional processing and lead to depression, it was hypothesized that a reduction of blue light using a fullerene filter will have positive effects on behavior. In contrast, very little is known about whether polyhydroxylated fullerene water complexes can influence brain activation and behavior. It was hypothesized they can interact via hydrogen bond exchange, but the exact mechanisms have yet to be determined.

3.1. Resting State fMRI

Resting state fMRI is a powerful tool to investigate changes in regional brain activity in response to long-term stimuli as opposed to paradigm induced functional MRI responses.

Changes in spectral composition by fullerene filtering, for 4 h daily, led to significantly decreased activation in the limbic brain area involved in emotional processing (amygdala) and the area involved in pain processing (periaqueductal gray), and increased activation of the thalamus, midbrain reticular nucleus and hindbrain region involved in wellbeing and subconscious functions (respiration, sleep, transition of wakefulness to sleep [55]), Figure 2A. There were no significant changes in cortical regions, suggesting only a subliminal, yet potentially important influence on behavior and sleep regulation. Daily treatment with 3HFWC led to significant activation of the periaqueductal gray, midbrain reticular nucleus and the superior colliculi, while significantly decreased activation was found in thalamus, hippocampus, hindbrain, amygdala and motor/somatosensory cortex, Figure 2B. Significantly increased activation of the periaqueductal gray, along with decreased activation of somatosensory cortex, suggested altered sensory and pain processing. The group that received dual treatment had significantly increased activation in the somatomotor, somatosensory, prelimbic, cingulate and retrosplenial cortex, periaqueductal gray and midbrain reticular nucleus, while decreased activation only in hindbrain and cerebellum, Figure 2C. Most of the activated brain regions were involved in higher cognitive functions, such as memory, spatial orientation, decision making, planning and emotions. However, behavioral testing did not extend to memory and spatial orientation. Peculiarly, mice treated with 3HFWC (with or without fullerene-filtered light) had almost perfect scores in nest building.

3.2. Body Weight and ECG and Blood Pressure

The body weight of individual animals was monitored weekly, for 7 weeks, with no statistically significant difference found between groups. Fullerene-filtered light treatment led to slightly increased body weight vs. controls, while 3HFWC led to slightly decreased body weight vs. control. The body weight of the dual treatment group was similar to controls, Figure 3A. There were no significant differences in blood pressure or any ECG abnormalities among different groups (data not shown).

3.3. Behavioral Testing

3.3.1. Elevated Plus Maze

The total distance travelled within the maze was not statistically different among any of the groups, Figure 3B. There were also no significant differences between times spent in different sections of the maze (open arms, closed arms, center) among different groups. The latency to enter open arms (OA) was significantly longer for the group that received dual treatment vs. the control or the group exposed to fullerene-filtered light (one-way ANOVA, with Fishers LSD post-hoc test, $p < 0.05$). This could indicate increased anxiety among mice on dual treatment.

3.3.2. Forced Swim Test and Tail Suspension Test

These two tests are used as a measure of depression-like phenotype. Reduction in latency to float and reduction in latency to stop struggling are correlated with depression. There were no statistically significant differences between groups in either latency to float, floating time or latency to stop struggling, Figure 3D–F. The group exposed to fullerene-filtered light trended toward slightly longer latency to start floating and increased struggling time, Figure 3D,F.

3.3.3. Dynamic Plantar Test

Mechanical pain sensitivity was tested using an automated von Frey test. No statistically significant differences in mechanical pain sensitivity were found among different groups.

3.3.4. Hot Plate Test

Treatment with 3HFWC alone, led to significantly decreased response latency in the hot plate test (increased sensitivity to thermal nociceptive stimulus) when compared with the control, fullerene-filtered light or combined treatment groups (one-way ANOVA, with Fishers LSD post-hoc test, $p < 0.05$).
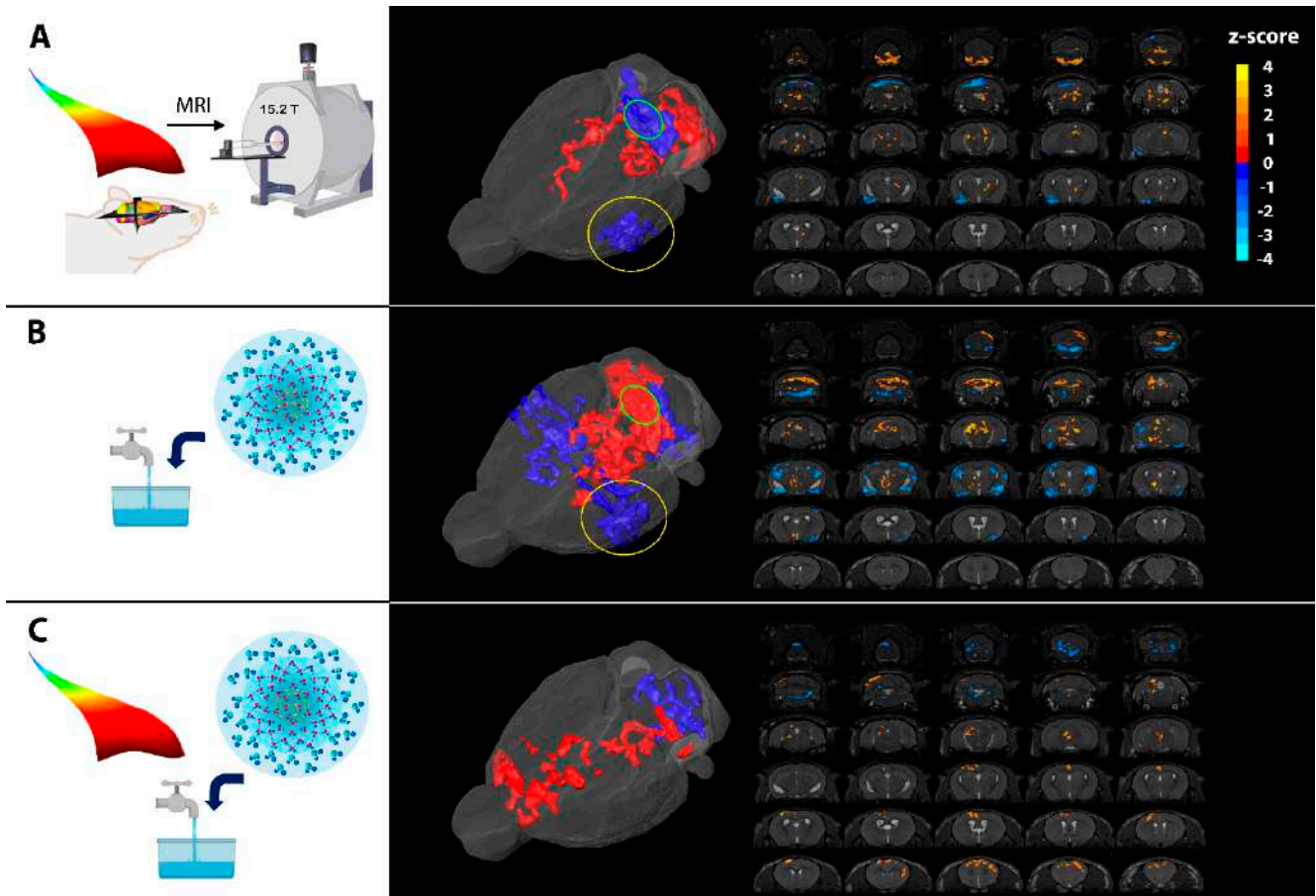

Figure 2. An illustration of experimental conditions for various treatment groups and resting state fMRI results. The resting state fMRI results are represented as 3D rendered brain and 2D coronal slices for each treatment group vs. control: (**A**) Fullerene-filtered light ($n = 5$), (**B**) 3HFWC ($n = 5$), (**C**) combined fullerene-filtered light and 3HFWC ($n = 5$). Brain regions with increased activation (vs. control) are pseudocolored red, and regions with decreased activation (vs. control) are pseudocolored blue. In 2D coronal slices, all pixels with statistically significant z-score are pseudocolored red (increased activation vs. control) or blue (decreased activation vs. control). The between-group comparison was conducted on z-scored ALFF maps, using a pairwise t-test followed by Gaussian Random Field (GRF) theory multiple comparison correction (voxel-level p-value = 0.05, cluster-level p-value = 0.05). The amygdala is outlined with yellow circle, and the periaqueductal gray with green circle.

3.3.5. Nest Building Test

Nest building is a naturally occurring behavior in mice, and participation in this activity is a simple indicator of wellbeing. It can also be used as a sensitive measure of acute illness, depression-like phenotype, or chronic mental health problems, all of which correlate with low nest scores [47,56]. Treatment with 3HFWC alone or together with fullerene-filtered light lead to significantly higher nest scores compared with the control group and the group treated with fullerene-filtered light alone (one-way ANOVA, with Fishers LSD post-hoc test, $p < 0.05$).
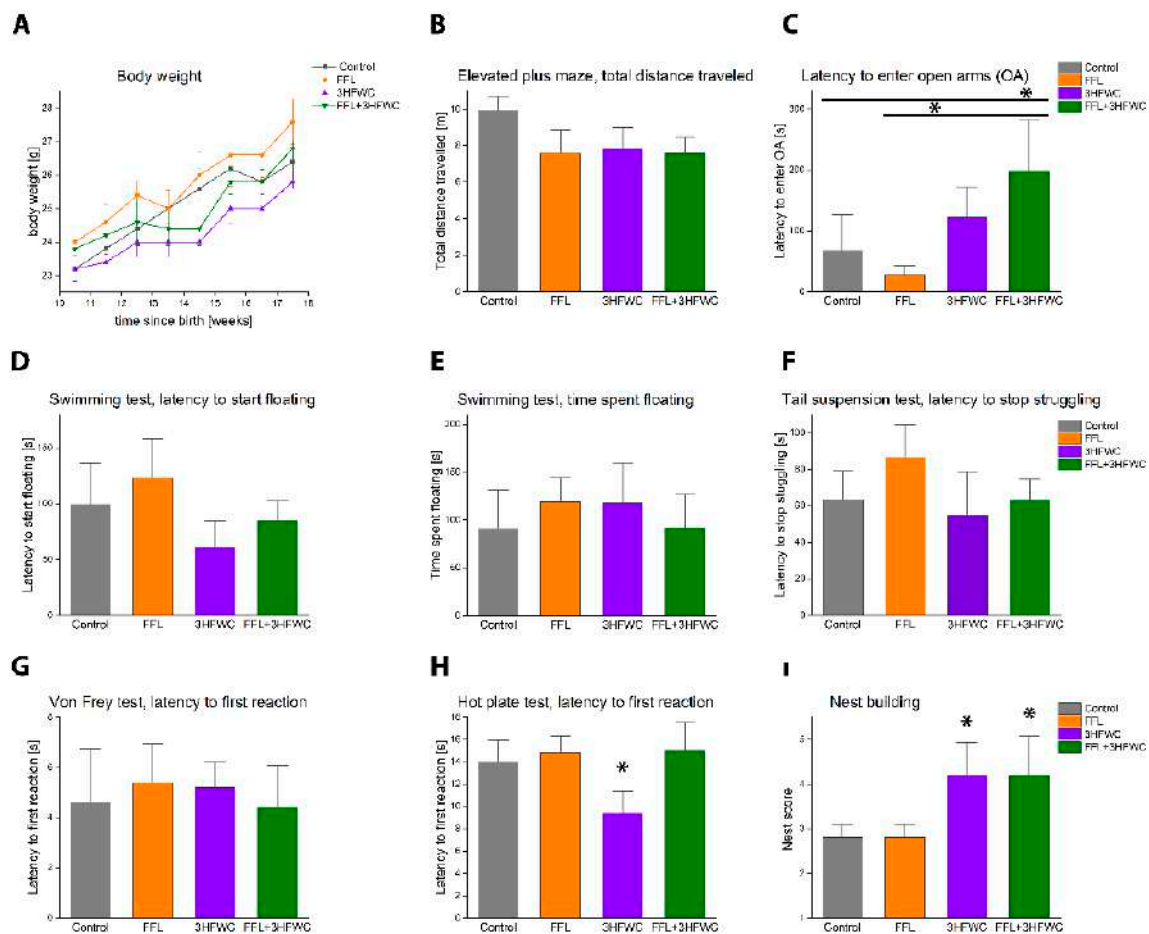
Figure 3. Results of behavioral testing, *n* = 5 mice per group. (**A**) The body weight measurements during 7 weeks of treatments, no significant difference was found. (**B**) Elevated plus maze, total distance traveled within the maze, no significant difference found. (**C**) Elevated plus maze, latency to enter open arms. Mice receiving dual treatment had significantly increased latency to enter open arms (vs. control and vs. fullerene-filtered light (FFL)). (**D**) Forced swimming test, latency to start floating, no significant difference was found. (**E**) Forced swimming test, time spent floating, no significant difference was found. (**F**) Tail suspension test, latency to stop struggling, no significant difference was found. (**G**) Mechanical pain sensitivity test (Von Frey test), latency to first reaction, no significant difference was found. (**H**) Hot plate test, latency to first reaction. Mice treated with 3HFWC had significantly decreased latency to first reaction vs. all other groups. (**I**) Nest building score, mice treated with 3HFWC and 3HFWC in combination with FFL had significantly higher nest building score compared with control and FFL group. FFL = fullerene-filtered light. (One-way ANOVA, * $p < 0.05$.)

3.4. Histopathology

Even though application of fullerene as an optical filter was not expected to lead to any significant toxicity, tissues from all treatment groups were subjected to histopathology. The 3HFWC, in the concentration range applied, was also not expected to be cytotoxic or neurotoxic. At the optical microscope level, no prominent degenerative, inflammatory or necrotizing lesions were evident for all sets of tissues (heart, lung, liver (Figure 4A), spleen, kidney (Figure 4B), bone, skeletal muscle and brain) examined regardless of the treatment group. From a neurotoxicity perspective, there were no major degenerative or inflammatory lesions in the evaluated brain regions of the examined slides, Figure 4C. There were no prominent regions of neuropil necrosis. No foci of apoptotic neurons and apoptotic glial cells (potentially consequent to tissue injury mediated by reactive oxygen species), regardless of treatments.
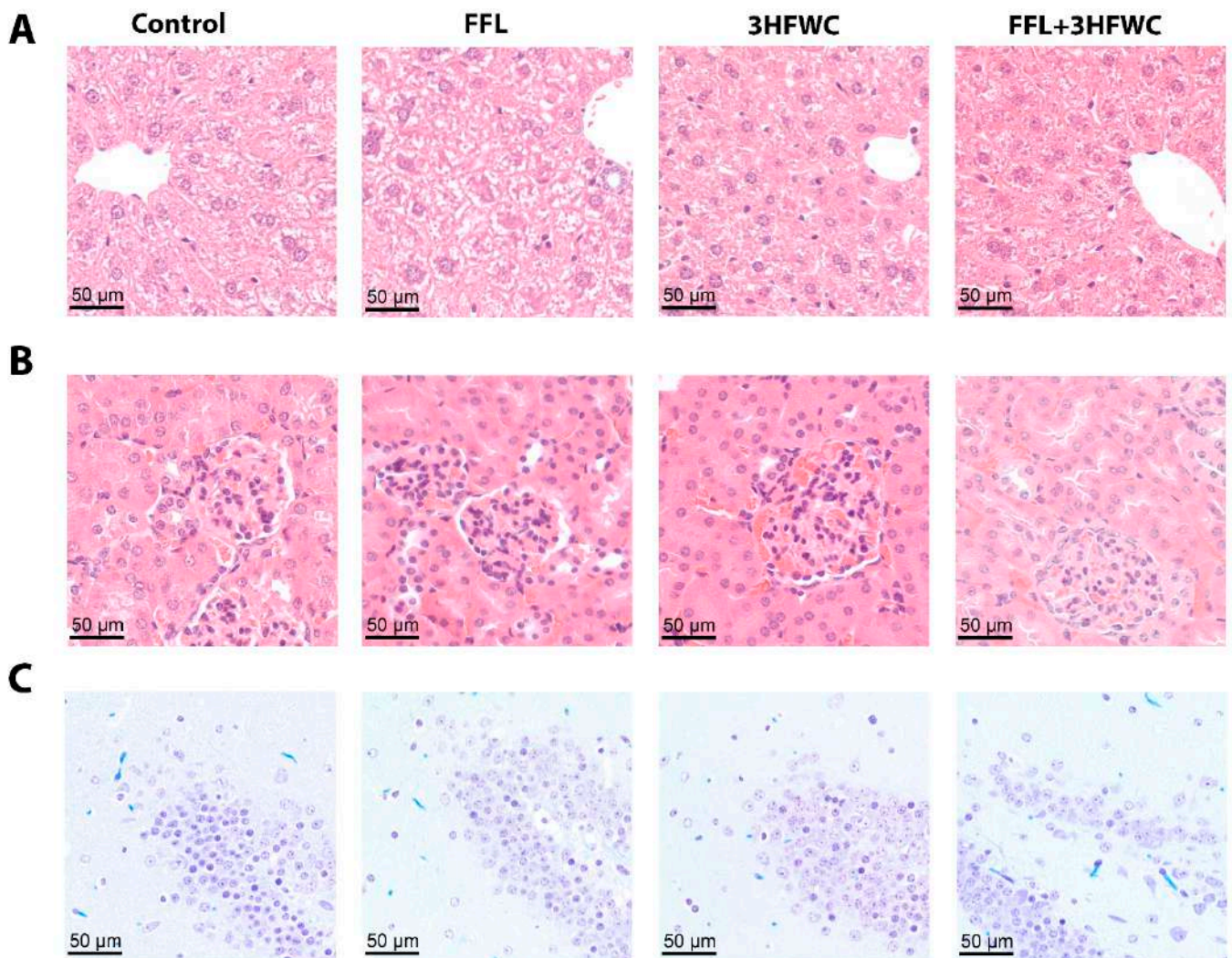
Figure 4. Representative H&E staining (40× magnification) for different treatment groups (**A**) liver sections, (**B**) kidney sections. No apparent cell necrosis, degenerative, inflammatory or necrotizing lesions were evident. (**C**) Representative Cresyl violet and luxol fast blue staining (40× magnification), from dentate gyrus of hippocampus (the most sensitive neurons to neurotoxins). No foci of apoptotic neurons or glial cells were found.

4. Discussion

Motivated and inspired by the minimally toxic and minimally invasive application of fullerene molecules, the results of the initial investigation of fullerene-filtered light and fullerene derivative 3HFWC complexes (non-toxic, concentration 0.15 g/L) on patterns of brain activation and the subsequent consequences on behavior are presented. Light therapies, in general, hold promise for therapeutic platforms, void of pharmacological interventions, and could significantly reduce treatment cost. It is, however, necessary to carefully evaluate potential spectral therapies for their effectiveness, which is not easy since it appears they can act at a subliminal level, and therefore influence unconscious behavior. Brain imaging studies offer a powerful approach to directly measure potential benefits and efficacy, by detecting associated changes in brain activity. Furthermore, it was demonstrated here that 3HFWC alone or in combination with fullerene-filtered light, can also significantly affect brain activation and behavior, and this should be kept in mind for the pharmaceutical agent development.

Because evidence from previous studies provided strong connections between the spectral quality of light and emotional responses, these behavioral studies were designed to test for anxiety and depression phenotypes. None of the treatment groups exhibited

a particular depression phenotype, while the group that received dual treatment had significantly increased latency to enter the open arms of the elevated water maze, which could be interpreted as increased anxiety. However, this group together with the group that received 3HFWC alone, had significantly higher scores in nest building, supporting wellbeing as well. The amygdala has been implicated in animal and human studies to play a critical role during stress responses, including memory formation and the initiation of adaptive coping responses [57,58]. Previous studies have demonstrated increased activation of the amygdala in response to anxiety, post-traumatic stress disorder (PTSD), social phobia, depression, impulsive aggression [59–62], chronic and visceral pain [63–65]. In particular, the emotional component related to anxiety and stress during a painful stimulus is thought to play a major role in the development of persistent pain and is the underlying etiology of disorders related to the gut-brain axis [66,67]. Prolonged exposure to stressors is expected to lead to activation of the amygdala as a coping response. A decreased activation of the amygdala was observed, in response to fullerene-filtered light and 3HFWC, supporting anti-depression and anti-anxiety phenotypes, as well as an application in adjunct pain therapy.

Increased sensitivity to an immediate thermal nociceptive stimulus (hot plate) was found with 3HFWC treatment. Resting state fMRI revealed increased activation of the periaqueductal gray, a major brain area involved in pain processing and modulation, and decreased activation of the somatosensory cortex, making interpretation of increased sensitivity counterintuitive. However, similarly found, was an increased activation of periaqueductal gray and decreased somatosensory activation in knockout mice with enhanced immediate nociceptive reaction, but long-term pain suppression (unpublished data). We speculate increased activation of periaqueductal gray to result in increased opioid release, and long-term pain suppression. Intriguingly, if increased sensitivity to nociceptive stimulus of the 3HFWC is compared with the dual treatment group, it can be argued that fullerene-filtered light in combined treatment restored sensitivity to control level, indicating an application for acute pain therapy. This is further supported by the evidence of increased activation of the prefrontal cortex and periaqueductal gray, two major areas involved in pain processing and pain modulation [68]. Increased activation of the periaqueductal gray area found with the addition of fullerene-filtered light, might be the reason for acute analgesia. Indeed, if pain is viewed as a complex blend of sensory, emotional and cognitive components [69], it can be concluded that the best analgesic treatment would be the combination of actions that will limit anxiety, stress and depression along with reduction of pain perception, such as the fullerene-filtered light and dual treatment presented here.

5. Conclusions

Daily exposure to fullerene-filtered light, led to decreased activation of the amygdala, suggesting it could be beneficial for a number of disorders associated with its increased activation (stress, anxiety, depression, PTSD, impulsive aggression, etc.). A combination of fullerene-filtered light with drinking water supplemented with 3HFWC, restored latency to first response to hot plate and activation of the prefrontal cortex as well as brain areas involved in cognitive functions and pain modulation. In conclusion, the present data indicate fullerene-filtered light is able to influence emotional response, and modulate pain perception, proposing its further use in stress and pain management.

Author Contributions: Conceptualization, J.L. and D.K.; synthesis of 3HFWC, M.S., Z.J., I.S. and V.M.; fMRI data analysis software, J.L. and M.G.; behavioral studies, J.H.; resources, D.K.; writing—original draft preparation, J.L.; writing—review and editing, J.L.; visualization, L.M.Z.; supervision, D.K.; project administration, D.K.; funding acquisition, J.L. All authors have read and agreed to the published version of the manuscript.

References

1. Kroto, H.W.; Heath, J.R.; O'Brien, S.C.; Curl, R.F.; E Smalley, R. C60: Buckminsterfullerene. *Nature* **1985**, *318*, 162–163. [CrossRef]
2. Bakry, R.; Vallant, R.M.; Najam-Ul-Haq, M.; Rainer, M.; Szabo, Z.; Huck, C.W.; Bonn, G.K. Medicinal Applications of Fullerenes. *Int. J. Nanomed.* **2007**, *2*, 639–649.
3. Andrievsky, G.V.; Bruskov, V.I.; Tykhomyrov, A.A.; Gudkov, S.V. Peculiarities of the Antioxidant and Radioprotective Effects of Hydrated C60 Fullerene Nanostuctures In Vitro and In Vivo. *Free. Radic. Biol. Med.* **2009**, *47*, 786–793. [CrossRef]
4. Dellinger, A.L.; Cunin, P.; Lee, D.; Kung, A.; Brooks, D.B.; Zhou, Z.; Nigrovic, P.A.; Kepley, C.L. Inhibition of Inflammatory Arthritis Using Fullerene Nanomaterials. *PLoS ONE* **2015**, *10*, e0126290. [CrossRef]
5. Prylutska, S.V.; Burlaka, A.P.; Klymenko, P.P.; Grynyuk, I.I.; Prylutskyy, Y.I.; Schütze, C.; Ritter, U. Using Water-Soluble C60 Fullerenes in Anticancer Therapy. *Cancer Nanotechnol.* **2011**, *2*, 105–110. [CrossRef] [PubMed]
6. Ngan, C.L.; Basri, M.; Tripathy, M.; Karjiban, R.A.; Abdul-Malek, E. Skin Intervention of Fullerene-Integrated Nanoemulsion in Structural and Collagen Regeneration Against Skin Aging. *Eur. J. Pharm. Sci.* **2015**, *70*, 22–28. [CrossRef] [PubMed]
7. Ito, S.; Itoga, K.; Yamato, M.; Akamatsu, H.; Okano, T. The Co-Application Effects of Fullerene and Ascorbic Acid on UV-B Irradiated Mouse Skin. *Toxicology* **2010**, *267*, 27–38. [CrossRef] [PubMed]
8. Chiang, L.Y.; Wang, L.-Y.; Swirczewski, J.W.; Soled, S.; Cameron, S. Efficient Synthesis of Polyhydroxylated Fullerene Derivatives via Hydrolysis of Polycyclosulfated Precursors. *J. Org. Chem.* **1994**, *59*, 3960–3968. [CrossRef]
9. Andrievsky, G.V.; Kosevich, M.V.; Vovk, O.M.; Shelkovsky, V.S.; Vashchenko, L.A. On the Production of an Aqueous Colloidal Solution of Fullerenes. *J. Chem. Soc. Chem. Commun.* **1995**, 1281–1282. [CrossRef]
10. Kokubo, K.; Matsubayashi, K.; Tategaki, H.; Takada, H.; Oshima, T. Facile Synthesis of Highly Water-Soluble Fullerenes More than Half-Covered by Hydroxyl Groups. *ACS Nano* **2008**, *2*, 327–333. [CrossRef]
11. LeGates, T.; Altimus, C.M.; Wang, H.; Lee, H.-K.; Yang, S.; Zhao, H.; Kirkwood, A.; Weber, E.T.; Hattar, S. Aberrant Light Directly Impairs Mood and Learning Through Melanopsin-Expressing Neurons. *Nature* **2012**, *491*, 594–598. [CrossRef] [PubMed]
12. Kim, J.; Jang, S.; Choe, H.K.; Chung, S.; Son, G.H.; Kim, A.K. Implications of Circadian Rhythm in Dopamine and Mood Regulation. *Mol. Cells* **2017**, *40*, 450–456. [CrossRef]
13. Provencio, I.; Rodriguez, I.R.; Jiang, G.; Hayes, W.P.; Moreira, E.F.; Rollag, M.D. A Novel Human Opsin in the Inner Retina. *J. Neurosci.* **2000**, *20*, 600–605. [CrossRef] [PubMed]
14. Hattar, S.; Liao, H.-W.; Takao, M.; Berson, D.M.; Yau, K.-W. Melanopsin-Containing Retinal Ganglion Cells: Architecture, Projections, and Intrinsic Photosensitivity. *Science* **2002**, *295*, 1065–1070. [CrossRef]
15. Berson, D.M.; Dunn, F.A.; Takao, M. Phototransduction by Retinal Ganglion Cells That Set the Circadian Clock. *Science* **2002**, *295*, 1070–1073. [CrossRef]
16. Hattar, S.; Kumar, M.; Park, A.; Tong, P.; Tung, J.; Yau, K.-W.; Berson, D.M. Central Projections of Melanopsin-Expressing Retinal Ganglion Cells in the Mouse. *J. Comp. Neurol.* **2006**, *497*, 326–349. [CrossRef] [PubMed]
17. Delwig, A.; Larsen, D.D.; Yasumura, D.; Yang, C.; Shah, N.M.; Copenhagen, D.R. Retinofugal Projections from Melanopsin-Expressing Retinal Ganglion Cells Revealed by Intraocular Injections of Cre-Dependent Virus. *PLoS ONE* **2016**, *11*, e0149501. [CrossRef]
18. Güler, A.D.; Ecker, J.L.; Lall, G.; Haq, S.; Altimus, C.M.; Liao, H.-W.; Barnard, A.R.; Cahill, H.; Badea, T.C.; Zhao, H.; et al. Melanopsin Cells are the Principal Conduits for Rod–Cone Input to Non-Image-Forming Vision. *Nature* **2008**, *453*, 102–105. [CrossRef]
19. Panda, S.; Sato, T.K.; Castrucci, A.M.; Rollag, M.D.; DeGrip, W.J.; Hogenesch, J.B.; Provencio, I.; Kay, S.A. Melanopsin (Opn4) Requirement for Normal Light-Induced Circadian Phase Shifting. *Science* **2002**, *298*, 2213–2216. [CrossRef]
20. Freedman, M.S.; Lucas, R.J.; Soni, B.; von Schantz, M.; Muñoz, M.; David-Gray, Z.; Foster, R. Regulation of Mammalian Circadian Behavior by Non-rod, Non-cone, Ocular Photoreceptors. *Science* **1999**, *284*, 502–504. [CrossRef]
21. Peirson, S.N.; Halford, S.; Foster, R.G. The Evolution of Irradiance Detection: Melanopsin and the Non-Visual Opsins. *Philos. Trans. R. Soc. B Biol. Sci.* **2009**, *364*, 2849–2865. [CrossRef]
22. Dacey, D.M.; Liao, H.-W.; Peterson, B.B.; Robinson, F.; Smith, V.C.; Pokorny, J.; Yau, K.-W.; Gamlin, P. Melanopsin-Expressing Ganglion Cells in Primate Retina Signal Colour and Irradiance and Project to the LGN. *Nature* **2005**, *433*, 749–754. [CrossRef]
23. Walmsley, L.; Hanna, L.; Mouland, J.W.; Martial, F.; West, A.; Smedley, A.; Bechtold, D.; Webb, A.R.; Lucas, R.J.; Brown, T.M. Colour as a Signal for Entraining the Mammalian Circadian Clock. *PLoS Biol.* **2015**, *13*, e1002127. [CrossRef] [PubMed]
24. Casper, R.F.; Rahman, S. Spectral Modulation of Light Wavelengths Using Optical Filters: Effect on Melatonin Secretion. *Fertil. Steril.* **2014**, *102*, 336–338. [CrossRef] [PubMed]

25. Reiter, R.J.; Tamura, H.; Tan, D.X.; Xu, X.-Y. Melatonin and The Circadian System: Contributions to Successful Female Reproduction. *Fertil. Steril.* **2014**, *102*, 321–328. [CrossRef] [PubMed]

26. Danilenko, K.V.; Sergeeva, O.Y. Immediate Effect of Blue-Enhanced Light on Reproductive Hormones in Women. *Neuro Endocrinol. Lett.* **2015**, *36*, 84–90.

27. Wulff, K.; Gatti, S.; Wettstein, J.G.; Foster, R.G. Sleep and Circadian Rhythm Disruption in Psychiatric and Neurodegenerative Disease. *Nat. Rev. Neurosci.* **2010**, *11*, 589–599. [CrossRef] [PubMed]

28. Imeraj, L.; Sonuga-Barke, E.; Antrop, I.; Roeyers, H.; Wiersema, R.; Bal, S.; Deboutte, D. Altered Circadian Profiles in Attention-Deficit/Hyperactivity Disorder: An Integrative Review and Theoretical Framework for Future Studies. *Neurosci. Biobehav. Rev.* **2012**, *36*, 1897–1919. [CrossRef]

29. Alloy, L.B.; Ng, T.H.; Titone, M.; Boland, E.M. Circadian Rhythm Dysregulation in Bipolar Spectrum Disorders. *Curr. Psychiatry Rep.* **2017**, *19*, 21. [CrossRef]

30. Wulff, K.; Dijk, D.-J.; Middleton, B.; Foster, R.G.; Joyce, E.M. Sleep and Circadian Rhythm Disruption in Schizophrenia. *Br. J. Psychiatry* **2012**, *200*, 308–316. [CrossRef]

31. Parekh, P.K.; Ozburn, A.R.; McClung, C.A. Circadian Clock Genes: Effects on Dopamine, Reward and Addiction. *Alcohol* **2015**, *49*, 341–349. [CrossRef] [PubMed]

32. Hu, H.; Kang, C.; Hou, X.; Zhang, Q.; Meng, Q.; Jiang, J.; Hao, W. Blue Light Deprivation Produces Depression-Like Responses in Mongolian Gerbils. *Front. Psychiatry* **2020**, *11*, 233. [CrossRef]

33. Lucas, R.J.; Douglas, R.H.; Foster, R.G. Characterization of an Ocular Photopigment Capable of Driving Pupillary Constriction in Mice. *Nat. Neurosci.* **2001**, *4*, 621–626. [CrossRef]

34. Inani, H.; Singhal, R.; Sharma, P.; Vishnoi, R.; Aggarwal, S.; Sharma, G. Effect of Low Fluence Radiation on Nanocomposite Thin Films of Cu Nanoparticles Embedded in Fullerene C 60. *Vacuum* **2017**, *142*, 5–12. [CrossRef]

35. Ogawa, S.; Lee, T.M.; Kay, A.R.; Tank, D.W. Brain Magnetic Resonance Imaging with Contrast Dependent on Blood Oxygenation. *Proc. Natl. Acad. Sci. USA* **1990**, *87*, 9868–9872. [CrossRef] [PubMed]

36. Ogawa, S.; Tank, D.W.; Menon, R.; Ellermann, J.; Kim, S.G.; Merkle, H.; Ugurbil, K. Intrinsic Signal Changes Accompanying Sensory Stimulation: Functional Brain Mapping with Magnetic Resonance Imaging. *Proc. Natl. Acad. Sci. USA* **1992**, *89*, 5951–5955. [CrossRef]

37. Biswal, B.; Yetkin, F.Z.; Haughton, V.M.; Hyde, J.S. Functional Connectivity in the Motor Cortex of Resting Human Brain Using Echo-Planar MRI. *Magn. Reson. Med.* **1995**, *34*, 537–541. [CrossRef] [PubMed]

38. Kropka, J.M.; Putz, K.W.; Pryamitsyn, V.; Ganesan, V.; Green, P.F. Origin of Dynamical Properties in PMMA−C60 Nanocomposites. *Macromolecules* **2007**, *40*, 5424–5432. [CrossRef]

39. Kawauchi, T.; Kumaki, J.; Kitaura, A.; Okoshi, K.; Kusanagi, H.; Kobayashi, K.; Sugai, T.; Shinohara, H.; Yashima, E. Encapsulation of Fullerenes in a Helical PMMA Cavity Leading to a Robust Processable Complex with a Macromolecular Helicity Memory. *Angew. Chem. Int. Ed.* **2008**, *47*, 515–519. [CrossRef]

40. Koruga, D. Optical Filter and Method of Manufacturing an Optical Filter. European Patent EP 3 469 406 B1; Bulletin 2020/33, 12 August 2020. US Patent 11,067,730 B2, 20 July 2021.

41. Stankovic, I.; Matija, L.; Jankov, M.; Jeftic, B.; Koruga, I.; Koruga, D. Optical and Structural Properties Of PMMA/C60 Composites with Different Concentrations of C60 Molecules and its Possible Applications. *J. Polym. Res.* **2020**, *27*, 224. [CrossRef]

42. Koruga, D. Composition of Matter Containing Harmonized Hydroxyl Modified Fullerene Substance. US Patent 8,058,483 B2, 15 November 2011.

43. Koruga, D. Compositions Comprising Hyper Harmonized Hydroxyl Modified Fullerene Substances. International Patent Application No. WO 2021/110234 A1, 10 June 2021.

44. Castagné, V.; Moser, P.; Roux, S.; Porsolt, R.D. Rodent Models of Depression: Forced Swim and Tail Suspension Behavioral Despair Tests in Rats and Mice. *Curr. Protoc.* **2011**, *55*, 8.10A.1–8.10A.14. [CrossRef] [PubMed]

45. Szabó, A.; Helyes, Z.; Sándor, K.; Bite, A.; Pintér, E.; Németh, J.; Bánvölgyi, A.; Bölcskei, K.; Elekes, K.; Szolcsányi, J. Role of Transient Receptor Potential Vanilloid 1 Receptors in Adjuvant-Induced Chronic Arthritis: In Vivo Study Using Gene-Deficient Mice. *J. Pharmacol. Exp. Ther.* **2005**, *314*, 111–119. [CrossRef]

46. El Maarouf, A.; Kolesnikov, Y.; Pasternak, G.; Rutishauser, U. Polysialic Acid-Induced Plasticity Reduces Neuropathic Insult to the Central Nervous System. *Proc. Natl. Acad. Sci. USA* **2005**, *102*, 11516–11520. [CrossRef]

47. Deacon, R.M.J. Assessing nest building in mice. *Nat. Protoc.* **2006**, *1*, 1117–1119. [CrossRef] [PubMed]

48. Yan, C. DPARSF: A MATLAB Toolbox for "Pipeline" Data Analysis of Resting-State fMRI. *Front. Syst. Neurosci.* **2010**, *4*, 13. [CrossRef]

49. Margulies, D.S.; Kelly, C.; Uddin, L.; Biswal, B.B.; Castellanos, F.X.; Milham, M.P. Mapping the Functional Connectivity of Anterior Cingulate Cortex. *NeuroImage* **2007**, *37*, 579–588. [CrossRef]

50. Friston, K.J.; Williams, S.; Howard, R.; Frackowiak, R.S.J.; Turner, R. Movement-Related Effects in fMRI Time-Series. *Magn. Reson. Med.* **1996**, *35*, 346–355. [CrossRef]

51. Yu-Feng, Z.; Yong, H.; Chao-Zhe, Z.; Qing-Jiu, C.; Man-Qiu, S.; Meng, L.; Li-Xia, T.; Tian-Zi, J. Altered Baseline Brain Activity in Children with ADHD Revealed by Resting-State Functional MRI. *Brain Dev.* **2007**, *29*, 83–91. [CrossRef] [PubMed]

52. Murphy, K.; Birn, R.M.; Handwerker, D.; Jones, T.B.; Bandettini, P.A. The Impact of Global Signal Regression on Resting State Correlations: Are Anti-Correlated Networks Introduced? *NeuroImage* **2009**, *44*, 893–905. [CrossRef]

53. Murphy, K.; Fox, M.D. Towards a Consensus Regarding Global Signal Regression for Resting State Functional Connectivity MRI. *NeuroImage* **2017**, *154*, 169–173. [CrossRef]

54. Saad, Z.S.; Gotts, S.J.; Murphy, K.; Chen, G.; Jo, H.J.; Martin, A.; Cox, R. Trouble at Rest: How Correlation Patterns and Group Differences Become Distorted After Global Signal Regression. *Brain Connect.* **2012**, *2*, 25–32. [CrossRef]

55. Crabtree, J.W. Functional Diversity of Thalamic Reticular Subnetworks. *Front. Syst. Neurosci.* **2018**, *12*, 41. [CrossRef]

56. Giménez-Llort, L.; Torres-Lista, V. Social Nesting, Animal Welfare, and Disease Monitoring. *Animals* **2021**, *11*, 1079. [CrossRef] [PubMed]

57. LeDoux, J.E. Emotion Circuits in the Brain. *Annu. Rev. Neurosci.* **2000**, *23*, 155–184. [CrossRef]

58. Hasler, G.; Fromm, S.; Alvarez, R.P.; Luckenbaugh, D.A.; Drevets, W.C.; Grillon, C. Cerebral Blood Flow in Immediate and Sustained Anxiety. *J. Neurosci.* **2007**, *27*, 6313–6319. [CrossRef]

59. Stein, M.B.; Simmons, A.N.; Feinstein, J.S.; Paulus, M.P. Increased Amygdala and Insula Activation During Emotion Processing in Anxiety-Prone Subjects. *Am. J. Psychiatry* **2007**, *164*, 318–327. [CrossRef] [PubMed]

60. Rauch, S.L.; Whalen, P.J.; Shin, L.M.; McInerney, S.C.; Macklin, M.L.; Lasko, N.B.; Orr, S.P.; Pitman, R.K. Exaggerated Amygdala Response to Masked Facial Stimuli in Posttraumatic Stress Disorder: A Functional MRI Study. *Biol. Psychiatry* **2000**, *47*, 769–776. [CrossRef]

61. Birbaumer, N.; Grodd, W.; Diedrich, O.; Klose, U.; Erb, M.; Lotze, M.; Schneider, F.; Weiss, U.; Flor, H. fMRI Reveals Amygdala Activation to Human Faces in Social Phobics. *NeuroReport* **1998**, *9*, 1223–1226. [CrossRef] [PubMed]

62. Coccaro, E.F.; McCloskey, M.; Fitzgerald, D.A.; Phan, K.L. Amygdala and Orbitofrontal Reactivity to Social Threat in Individuals with Impulsive Aggression. *Biol. Psychiatry* **2007**, *62*, 168–178. [CrossRef]

63. Johnson, A.C.; Myers, B.; Lazovic, J.; Towner, R.; Meerveld, B.G.-V. Brain Activation in Response to Visceral Stimulation in Rats with Amygdala Implants of Corticosterone: An fMRI Study. *PLoS ONE* **2010**, *5*, e8573. [CrossRef] [PubMed]

64. Lazovic, J.; Wrzos, H.F.; Yang, Q.X.; Collins, C.; Smith, M.B.; Norgren, R.; Matyas, K.; Ouyang, A. Regional Activation in the Rat Brain During Visceral Stimulation Detected by C-Fos Expression and fMRI. *Neurogastroenterol. Motil.* **2005**, *17*, 548–556. [CrossRef] [PubMed]

65. Simons, L.E.; Moulton, E.; Linnman, C.; Carpino, E.; Becerra, L.; Borsook, D. The Human Amygdala and Pain: Evidence from Neuroimaging. *Hum. Brain Mapp.* **2014**, *35*, 527–538. [CrossRef]

66. Keefe, F.J.; Lumley, M.; Anderson, T.; Lynch, T.; Carson, K.L. Pain and Emotion: New Research Directions. *J. Clin. Psychol.* **2001**, *57*, 587–607. [CrossRef]

67. Mayer, E.A. Gut Feelings: The Emerging Biology of Gut–Brain Communication. *Nat. Rev. Neurosci.* **2011**, *12*, 453–466. [CrossRef] [PubMed]

68. Ong, W.-Y.; Stohler, C.S.; Herr, D.R. Role of the Prefrontal Cortex in Pain Processing. *Mol. Neurobiol.* **2019**, *56*, 1137–1166. [CrossRef] [PubMed]

69. Melzack, R.; Wall, P.D. Pain Mechanisms: A New Theory. *Science* **1965**, *150*, 971–978. [CrossRef]